On the two-way diamond relay channel with lattice-based Compress-and-Forward

Anne Savard and Laurent Clavier
IMT Lille Douai, Univ. Lille, CNRS, UMR 8520 - IEMN
F-59000 Lille, France
Email: (anne.savard, laurent.clavier)@imt-lille-douai.fr

***Abstract*—This paper focuses on the full-duplex Gaussian two-way diamond relay channel (TWDRC), where two users wish to exchange their messages with the help of two relays, when one relay performs a lattice-based Compress-and-Forward (CF) scheme. The other relay performs either Decode-and-Forward (DF), Amplify-and-Forward (AF) or a lattice-based CF scheme. We start by proposing a novel lattice-based CF/CF scheme, where both relays perform CF. As opposed to the single relay case, two main challenges arise: the quantization rate region is constrained by two Multiple Access Channel (MAC) rate regions, and each user has to combine two noisy observations to decode the sent message. These challenges are tackled by exploiting MAC techniques and Maximum Ratio Combining methods, which are used to combine the two noisy observations. We then characterize a general achievable rate region when one relay sends a version of both users' messages (eventually noisy), which encompasses both AF and DF, and the other relay performs CF and derive the corresponding achievable rate regions. Finally, the three proposed relaying schemes are compared via numerical evaluations. Clearly, the position of both relays has an impact on the best relaying strategy.**

I. INTRODUCTION

With the growing demand for higher data rates and the increasing number of communicating devices, one widely accepted solution for the next generation of wireless communication systems relies on cooperative communication. The relay channel [13], in which one user wishes to send messages to a destination with the help of one relay is the easiest example of such a cooperative communication. Achievable rates using Compress-and-Forward (CF) or Decode-and-Forward (DF) have been characterized for this channel model in [2]. Cooperative two-way communication, in which two users wish to exchange their messages with the help of one (two-way relay channel) or more relays is a natural extension of the relay channel.

Consider a bi-directionnal communication between two users, where two relays are available to help this communication. This configuration is known as the two-way diamond relay channel (TWDRC). In this paper, we assume additive white Gaussian noise (AWGN) channels with a path loss proportional to the link distance and consider a full-duplex case. Previous work has been done on the half-duplex Gaussian diamond relay channel [7], [3]. Authors in [1] provided some results for the deterministic TWDRC as well as for the Gaussian TWDRC, where they assumed that the channel gains on the links from one relay to both users are the same. To the best of our knowledge, this work is one of the first attempts to focus on the full-duplex Gaussian model, where no constraints apply on the channel gains. This study brings us closer to a general cooperative communication with multiple users and multiple relays, which could represent a device to device communication for 5G communications. We propose to study the case where one relay is not able to decode both users' messages, but is able to perform a novel lattice-based CF scheme. Three achievable rate region are derived: CF/CF, where the other relay performs a lattice-based CF scheme, DF/CF, where it performs a DF scheme and AF/CF, where an AF scheme is used at the second relay. Lattice coding is an interesting tool, especially for AWGN channels since it achieves capacity with a low decoding complexity and it has been shown to achieve various rate regions for the Gaussian relay channel [5], [12], as well as for the Gaussian two-way relay channel [4], [9], or for the Gaussian multiway relay channel with direct links [10].

The rest of the paper is organized as follows: Section II describes the Gaussian TWDRC model. For the sake of completeness, Section III introduces some basic notions on lattice coding. Section IV presents our main results, starting with the achievable rate region under the lattice-based CF/CF scheme. Then, a general achievable rate region when one relay performs CF and when each user has access to both a compressed version and a noisy observation of the other user's message is derived and finally the achievable rate regions when the other relay performs either DF or AF, is provided. Section V outlines the proofs of our main results and numerical results are given in Section VI. Finally, Section VII concludes the paper.

II. GAUSSIAN TWO-WAY DIAMOND RELAY CHANNEL AND NOTATION

The studied model, the TWDRC, in which two users want to exchange their messages with the help of two relays, is depicted in Fig. 1. In the AWGN case, user $U_i, i \in \{1,2\}$ sends X_i of average power P_i and relay $R_j, j \in \{1,2\}$ sends X_{R_j} of average power P_{R_j}. The received signals at relay 1 and relay 2 are

$$Y_{R_1} = h_1 X_1 + h_2 X_2 + Z_{R_1},$$
$$Y_{R_2} = g_1 X_1 + g_2 X_2 + Z_{R_2},$$

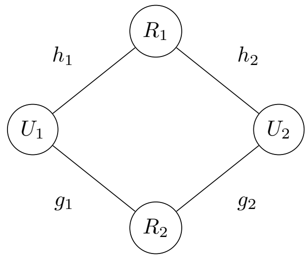

Fig. 1. Diamond relay channel.

and the received signals at user $U_i, i \in \{1,2\}$ are

$$Y_i = h_i X_{R_1} + g_i X_{R_2} + Z_i,$$

where Z_i and Z_{R_j} are Gaussian noises of variance N_i and N_{R_j}, respectively. We consider restricted encoders, such that the nodes' inputs depend only on their own current messages and not on past symbols.

Without loss of generality, we assume that relay R_2 always perform a lattice-based CF scheme.

The following notations will be used throughout the paper. $C(x)$ denotes the capacity function: $C(x) = \frac{1}{2}\log_2(1+x)$. For $i \in \{1,2\}, i' = \{1,2\} \setminus i$, $\overline{x}$ denotes $\overline{x} = 1-x$ and $\sigma_{R_1}^2 = h_1^2 P_1 + h_2^2 P_2 + N_{R_1}$. The received signal at relay R_j can be written as the sum of an unknown part U_{ij} of power σ_{ij}^2 and an available side information S_{ij} with respect to user U_i such that:

$$\begin{aligned} Y_{R_1} &= S_{11} + U_{11} = S_{21} + U_{21}, \\ Y_{R_2} &= S_{12} + U_{12} = S_{22} + U_{22}, \text{ with} \end{aligned}$$

$$\begin{aligned} S_{i1} = h_i X_i,\ U_{i1} = h_{i'} X_{i'} + Z_{R_1},\ \sigma_{i1}^2 = h_{i'}^2 P_{i'} + N_{R_1}, \\ S_{i2} = g_i X_i,\ U_{i2} = g_{i'} X_{i'} + Z_{R_2},\ \sigma_{i2}^2 = g_{i'}^2 P_{i'} + N_{R_2}. \end{aligned}$$

III. Lattice coding

We start by providing some definitions and notions on lattice coding, which are needed to derive our lattice-based relaying scheme. For a full treatment on the topic, the interested reader is referred to [14].

A lattice $\Lambda \subset \mathbb{R}^n$ is a discrete additive subgroup of $\mathbb{R}^n$. The *lattice quantizer* Q_Λ maps any point $x \in \mathbb{R}^n$ to the nearest lattice point: $Q_\Lambda(x) = \arg\min_{\lambda \in \Lambda} ||x – \lambda||$, where $||\cdot||$ denotes the Euclidean norm. The *fundamental Voronoi region* $\mathcal{V}$ of the lattice Λ is formed by all points that are closer to the origin than to any other lattice point: $\mathcal{V} = \{x \in \mathbb{R}^n | Q_\Lambda(x) = 0\}$. The quantization error, which is ensured to lie in $\mathcal{V}$ is obtained by the *modulo* Λ *operation*: $x \bmod \Lambda = x - Q_\Lambda(x)$. This operation enjoys the distributivity law: $\forall x, y \in \mathbb{R}^n$, $\big[[x] \bmod \Lambda + y\big] \bmod \Lambda = \big[x + y\big] \bmod \Lambda$. The *second moment per dimension* $\sigma^2(\Lambda)$ defines the average power of the lattice Λ: $\sigma^2(\Lambda) = \frac{1}{nV}\int_{\mathcal{V}} ||x||^2 dx$, where V is the volume of the fundamental Voronoi region of Λ.

Good lattice codebooks are obtained with the help of two nested lattices Λ and Λ_c, where $\Lambda \subseteq \Lambda_c$. These lattices are chosen such that Λ is both Rogers [8]- and Poltyrev [6]-good and Λ_c is Poltyrev-good.

IV. Achievable rate regions over the Gaussian TWDRC

In this section, we provide our main results for the TWDRC.

A. Achievable rate region with CF/CF

We first derive an achievable lattice-based CF/CF rate region over the Gaussian TWDRC.

Proposition 1 *For any quantization rates R_{q_1} and R_{q_2} satisfying the constraints (2)-(3) given below, the achievable rate region over the Gaussian TWDRC under a lattice-based CF/CF scheme is given by*

$$R_i^{CF/CF} \leq C\left(\frac{h_i^2 P_i}{N_{R_1} + \frac{\max\{\sigma_{11}^2, \sigma_{21}^2\}}{2^{2R_{q_1}}-1}} + \frac{g_i^2 P_i}{N_{R_2} + \frac{\max\{\sigma_{12}^2, \sigma_{22}^2\}}{2^{2R_{q_2}}-1}}\right). \quad (1)$$

The achievable quantization rate region, depicted on Fig. 2, is given as

$$R_{q_1} \leq C\left(P_{R_1} \min_i \frac{h_i^2}{N_i}\right), R_{q_2} \leq C\left(P_{R_2} \min_i \frac{g_i^2}{N_i}\right) \quad (2)$$

$$R_{q_1} + R_{q_2} \leq C\left(\min_i \frac{h_i^2 P_{R_1} + g_i^2 P_{R_2}}{N_i}\right). \quad (3)$$

Proof: The proof of the achievable CF/CF rate region is based on Wyner-Ziv decoding and Maximum Ratio combining (MRC) and the proof of the achievable quantization rate region is based on perfect decoding of both quantization indexes at both users. Both parts will be outlined in Section V-A. ■

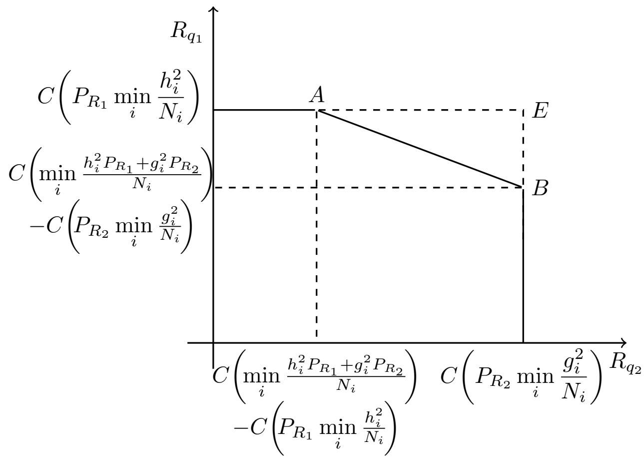

Fig. 2. Quantization rate region

Note that if the most restricting quantization constraints are the individual ones (eq. (2)), i.e. if

$$C\left(P_{R_1} \min_i \frac{h_i^2}{N_i}\right) + C\left(P_{R_2} \min_j \frac{g_j^2}{N_j}\right) \leq C\left(\min_k \frac{h_k^2 P_{R_1} + g_k^2 P_{R_2}}{N_k}\right) \quad (4)$$

then the achievable quantization rate region is shaped as a rectangle with corner point E. If, instead, the most restricting quantization constraint is the sum-constraint (3), then the achievable quantization rate region is shaped as a pentagon with two corner points A and B.

Since both $R_1^{CF/CF}$ and $R_2^{CF/CF}$ are increasing functions of R_{q_1} and R_{q_2}, the quantization rates must be chosen as large as possible. Thus, if (4) is satisfied, the optimal point in the quantization rate region is corner point E. The next proposition provides some conditions for the point E to be achievable as well as the achievable CF/CF rate region.

Proposition 2 *If the system parameters meet one of the three conditions below, then the corner point E in the quantization rate region (Fig. 2) is achievable: $\forall i \in \{1,2\}$,*

$$\begin{aligned}[C_1] &: h_i^2 g_i^2 P_{R_1} P_{R_2} N_{i'} \leq P_{R_1} N_i (h_{i'}^2 N_i - h_i^2 N_{i'}) \\ &\qquad + P_{R_2} N_i (g_{i'}^2 N_i - g_i^2 N_{i'}) \\ [C_2] &: h_i^2 (N_{i'} + g_{i'}^2 P_{R_2}) \leq h_{i'}^2 N_i \\ [C_3] &: g_{i'}^2 (N_i + h_i^2 P_{R_1}) \leq g_i^2 N_{i'}.\end{aligned}$$

The achievable rate region using the lattice-based CF/CF scheme is thus given by

$$R_i^{CF/CF} \leq C\left(\frac{h_i^2 P_i}{N_{R_1} + \frac{\max\{\sigma_{11}^2, \sigma_{21}^2\}}{P_{R_1} \min_i \frac{h_i^2}{N_i}}} + \frac{g_i^2 P_i}{N_{R_2} + \frac{\max\{\sigma_{12}^2, \sigma_{22}^2\}}{P_{R_2} \min_j \frac{g_j^2}{N_j}}}\right)$$

Proof: The three cases are obtained by considering $i = j \neq k$, $j = k \neq i$ and $i = k \neq j$ in (4). The case $i = j = k$ leads to a contradiction and is thus not possible. Replacing the quantization rates associated with corner point E into (1) yields the result. ■

On the other hand, if the most restricting quantization constraint is the sum-constraint, the largest CF rates are achieved for some quantization point lying on the line between the corner point A and B. However, a specific operating point cannot be easily determined, since it depends on all channel gains, noise and signal powers. Working at corner point A, resp. corner point B, provides an advantage to the quantization done at relay 1, resp. relay 2 (over the quantization done at the other relay), but no further conclusion can be made on $R_1^{CF/CF}$, $R_2^{CF/CF}$, or their sum, because of the non-trivial impact/dependence on all system parameters.

Note that having two relays enlarges the achievable rate region compared to the single relay case. Nevertheless, if only one relay is available, replacing for instance $g_i = 0, i \in \{1,2\}$ and $R_{q_2} = 0$ into Proposition 1, our achievable rate region reduces to the generalization of the results obtained in [11] to the full-duplex case.

B. Achievable rate region with DF/CF and AF/CF

We now provide the achievable rate region when a lattice-based DF/CF, respectively a lattice-based AF/CF, is used over the Gaussian TWDRC, where relay R_1 performs DF, respectively AF, and relay R_2 performs a lattice-based CF.

We start by providing a general achievable rate region when relay R_1 sends a message of the form $X_{R_1} = \rho_1 X_1 + \rho_2 X_2 + \rho_3 Z_{R_1}$, where ρ_i are scaling factors chosen based on the relaying scheme performed and are such that the average power constraint at relay R_1 is satisfied, yielding $\rho_1^2 P_1 + \rho_2^2 P_2 + \rho_3^2 N_{R_1} = P_{R_1}$. This specific form of X_{R_1} is a general form encompassing both DF and AF, as we will see later on.

In the next Proposition, we only assume that the signal sent by R_1 is of the form above, and don't take into account additional constraints that could apply on both users' rate and/or their sum, in order for relay R_1 to be able to send such a signal. The two following corollaries present the achievable rate region when relay R_1 performs DF, respectively AF.

Proposition 3 *If relay R_1 sends a signal of the general form $X_{R_1} = \rho_1 X_1 + \rho_2 X_2 + \rho_3 Z_{R_1}$ and relay R_2 performs a lattice-based CF, the following rate region is achievable*

$$R_1^g \leq C\left(\frac{g_1^2 P_1}{N_{R_2} + D} + \frac{h_2^2 \rho_1^2 P_1}{N_{eq_2}}\right), R_2^g \leq C\left(\frac{g_2^2 P_2}{N_{R_2} + D} + \frac{h_1^2 \rho_2^2 P_2}{N_{eq_1}}\right),$$

where D and N_{eq_i} are defined as $N_{eq_i} = h_i^2 \rho_3^2 N_{R_1} + N_i$ and

$$D = \frac{N_{R_2} + \max\left\{\frac{g_1^2 P_1 N_{eq_2}}{h_2^2 \rho_1^2 P_1 + N_{eq_2}}; \frac{g_2^2 P_2 N_{eq_1}}{h_1^2 \rho_2^2 P_2 + N_{eq_1}}\right\}}{\min\left\{\frac{g_1^2 P_{R_2}}{N_{eq_1} + h_1^2 \rho_2^2 P_2}; \frac{g_2^2 P_{R_2}}{N_{eq_2} + h_2^2 \rho_1^2 P_1}\right\}}.$$

Proof: The proof of this achievable rate region is based on block Markov coding, Wyner-Ziv coding and MRC and the outline will be presented in Section V-B. ■

Corollary 1 *The achievable rate region over the Gaussian TWDRC under a lattice-based DF/CF scheme is given by*

$$\begin{aligned}R_1^{DF/CF} &\leq \min\left\{C\left(\frac{h_1^2 P_1}{N_{R_1}}\right); C\left(\frac{g_1^2 P_1}{N_{R_2} + D} + \frac{h_2^2 \gamma_1^2 P_{R_1}}{N_2}\right)\right\}, \\ R_2^{DF/CF} &\leq \min\left\{C\left(\frac{h_2^2 P_2}{N_{R_1}}\right); C\left(\frac{g_2^2 P_2}{N_{R_2} + D} + \frac{h_1^2 \overline{\gamma_1^2} P_{R_1}}{N_1}\right)\right\}, \\ R_1^{DF/CF} &+ R_2^{DF/CF} \leq C\left(\frac{h_1^2 P_1 + h_2^2 P_2}{N_{R_1}}\right), \text{ where}\end{aligned}$$

$$D = \frac{\max\left\{\frac{g_2^2 P_2 N_1}{h_1^2 \overline{\gamma_1^2} P_{R_1} + N_1}; \frac{g_1^2 P_1 N_2}{h_2^2 \gamma_1^2 P_{R_1} + N_2}\right\} + N_{R_2}}{\min\left\{\frac{g_1^2 P_{R_2}}{N_1 + h_1^2 \overline{\gamma_1^2} P_{R_1}}; \frac{g_2^2 P_{R_2}}{N_2 + h_2^2 \gamma_1^2 P_{R_1}}\right\}}.$$

$0 \leq \gamma_1 \leq 1$ controls the power trade-off at relay R_1 between the part intended to user U_1 and user U_2.

Proof: During block b, the relay R_1 decodes both $X_1(b)$ and $X_2(b)$, yielding the additional MAC constraint on $R_1^{DF/CF}$ and $R_2^{DF/CF}$ given in Corollary 1 and allocates a fraction γ_1^2 of its available power for the transmission of $X_1(b)$ and the rest for $X_2(b)$ and sends $X_{R_1}^{DF}(b) = \sqrt{\frac{\gamma_1^2 P_{R_1}}{P_1}} X_1(b-1) + \sqrt{\frac{\overline{\gamma_1^2} P_{R_1}}{P_2}} X_2(b-1)$. Thus, $\rho_1 = \sqrt{\frac{\gamma_1^2 P_{R_1}}{P_1}}$, $\rho_2 = \sqrt{\frac{\overline{\gamma_1^2} P_{R_1}}{P_2}}$, $\rho_3 = 0$. ■

Corollary 2 *The achievable rate region over the Gaussian TWDRC under a lattice-based AF/CF scheme is given by*

$$R_i^{AF/CF} \leq C\left(\frac{h_1^2 h_2^2 P_i \frac{P_{R_1}}{\sigma^2_{R_1}}}{N_{eq_{i'}}} + \frac{g_i^2 P_i}{N_{R_2}+D}\right),$$

where N_{eq_i} *and* D *are given as* $N_{eq_i} = h_i^2 P_{R_1}\dfrac{N_{R_1}}{\sigma^2_{R_1}} + N_i$,

$$D = \frac{N_{R_2} + \max_{i\in\{1;2\}}\left\{\frac{g_i^2 h_{i'}^2 P_{R_1} P_i N_{R_1} + N_{i'} g_i^2 P_i \sigma^2_{R_1}}{h_{i'}^2 P_{R_1}\sigma^2_{i'1} + N_{i'}\sigma^2_{R_1}}\right\}}{\min\left\{\frac{g_1^2 P_{R_2}}{h_1^2 P_{R_1}\frac{\sigma^2_{11}}{\sigma^2_{R_1}} + N_1}; \frac{g_2^2 P_{R_2}}{h_2^2 P_{R_1}\frac{\sigma^2_{21}}{\sigma^2_{R_1}} + N_2}\right\}}.$$

Proof: During block b, relay R_1 sends a scaled version of its received signal satisfying its power constraints as $X_{R_1}^{AF}(b) = \sqrt{\frac{P_{R_1}}{\sigma^2_{R_1}}}\left(h_1 X_1(b-1) + h_2 X_2(b-1) + Z_{R_1}(b-1)\right)$. Thus, $\rho_1 = \sqrt{\frac{P_{R_1}}{\sigma^2_{R_1}}} h_1$, $\rho_2 = \sqrt{\frac{P_{R_1}}{\sigma^2_{R_1}}} h_2$, $\rho_3 = \sqrt{\frac{P_{R_1}}{\sigma^2_{R_1}}}$. ■

V. Proof of Proposition 1 and Proposition 3

Both proofs rely on lattice coding and decoding and are based on block Markov coding. Lattice-based codebooks are given as $\mathcal{C}_i = \{\Lambda_{c_i} \cap \mathcal{V}_i\}$, where $\Lambda_i \subseteq \Lambda_{c_i}$ for $i \in \{1, 2, Q_1, Q_2, R_1, R_2\}$, where Q_i denotes the quantization. For $i \in \{1, 2, R_1, R_2\}$, Λ_{c_i} is Poltyrev-good and Λ_i is both Rogers- and Poltyrev-good. Λ_{Q_i} is Poltyrev-good and Λ_{cQ_i} is Rogers-good, $i \in \{1, 2\}$. The quantization rate is defined as $R_{q_i} = \frac{1}{2}\log_2\left(\frac{\sigma^2(\Lambda_{Q_i})}{\sigma^2(\Lambda_{cQ_i})}\right)$. The choice for $\sigma^2(\Lambda_{cQ_i})$ and $\sigma^2(\Lambda_{Q_i})$ will be specified later in the proofs. Throughout the proof, u_i is a dither uniformly distributed over $\mathcal{V}_i$ and known by all nodes.

Due to space limitation, we only outline the proofs.

A. Proof of Proposition 1

The proof and Proposition 1 is inspired from [11], in which the authors proposed a lattice-based two-way CF scheme for the half-duplex two-way relay channel, assuming that only one relay helps the communication. The main differences here are the full-duplex nodes and the presence of a second relay. Thus, one key challenge is how to combine the two noisy observations obtained from the two relays. We propose to combine the two using MRC since it is known to be the optimal combiner under AWGN.

1) Encoding at each user: Codebooks $\mathcal{C}_i$ are build on nested lattices, where to ensure the power constraints, we choose $\sigma^2(\Lambda_i) = P_i$ and Λ_{c_i} such that $|\mathcal{C}_i| = 2^{nR_i^{CF/CF}}$. During block b, each user sends $X_i(b) = [c_i(b) + u_i(b)] \bmod \Lambda_i$.

2) Encoding at each relay: The quantization codebooks are given by $\mathcal{C}_{q_i}$. The codebooks for each relay are given by $\mathcal{C}_{R_i}$, where in order to ensure the power constraints, we choose $\sigma^2(\Lambda_{R_i}) = P_{R_i}$. Each compression index j_i is mapped to one codeword c_{R_i}, thus Λ_{R_i} is chosen such that $|\mathcal{C}_{R_i}| = 2^{nR_{q_i}}$. During transmission block b, the relays send

$$X_{R_i}(b) = [c_{R_i}(j_i(b-1)) + u_{R_i}(b)] \bmod \Lambda_{R_i}.$$

3) Quantization: As depicted in Fig. 3, relay quantizes $Y_{R_i}(b)$ to $j_i(b) = [\beta_i Y_{R_i}(b) + u_{cQ_i}(b) + E_{cQ_i}(b)] \bmod \Lambda_{Q_i}$, where β_i is a scaling factor and $E_{cQ_i}(b)$ is the quantization error.

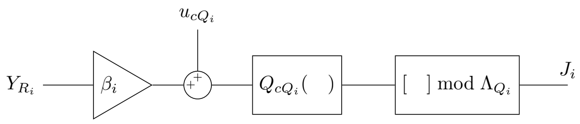

Fig. 3. Quantization at the relay.

4) Decoding at user U_1: During block b, user U_1 starts by decoding both quantization indexes as long as

$$R_{q_1} \leq C\left(\frac{h_1^2 P_{R_1}}{N_1}\right), R_{q_2} \leq C\left(\frac{g_1^2 P_{R_2}}{N_1}\right), R_{q_1} + R_{q_2} \leq C\left(\frac{h_1^2 P_{R_1} + g_1^2 P_{R_2}}{N_1}\right).$$

The decoding of $X_2(b-1)$ is performed in a Wyner-Ziv fashion as depicted in Fig. 4. User U_1 estimates $\widehat{U}_{1i}(b-1)$ using the decoded quantization index $j_i(b-1)$ and the side information $S_{1i}(b-1)$ as $\widehat{U}_{1i}(b-1) = \gamma_{1i}\beta_i U_{1i}(b-1) + \gamma_{1i} E_{cQ_i}(b-1)$, which requires that $\sigma^2(\Lambda_{Q_i}) \geq \beta_i^2 \sigma^2_{1i} + \sigma^2(\Lambda_{cQ_i})$. In order to recover $X_2(b-1)$, user U_1 combines $\widehat{U}_{11}(b-1)$ and $\widehat{U}_{12}(b-1)$ using MRC and perfect decoding is possible as long as

$$R_2^{CF/CF} \leq C\left(\frac{\beta_1^2 h_2^2 P_2}{\beta_1^2 N_{R_1} + \sigma^2(\Lambda_{cQ_1})} + \frac{\beta_2^2 g_2^2 P_2}{\beta_2^2 N_{R_2} + \sigma^2(\Lambda_{cQ_2})}\right). \quad (5)$$

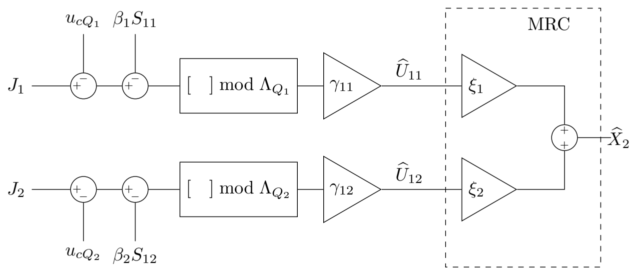

Fig. 4. Decoding step at user U_1.

5) Decoding at user U_2: Following the same arguments as for user U_1, perfect decoding at user U_2 requires that

$$R_{q_1} \leq C\left(\frac{h_2^2 P_{R_1}}{N_2}\right), R_{q_2} \leq C\left(\frac{g_2^2 P_{R_2}}{N_2}\right), R_{q_1} + R_{q_2} \leq C\left(\frac{h_2^2 P_{R_1} + g_2^2 P_{R_2}}{N_2}\right)$$

$\sigma^2(\Lambda_{Q_i}) \geq \beta_i^2 \sigma^2_{2i} + \sigma^2(\Lambda_{cQ_i})$ and

$$R_1^{CF/CF} \leq C\left(\frac{\beta_1^2 h_1^2 P_1}{\beta_1^2 N_{R_1} + \sigma^2(\Lambda_{cQ_1})} + \frac{\beta_2^2 g_1^2 P_1}{\beta_2^2 N_{R_2} + \sigma^2(\Lambda_{cQ_2})}\right). \quad (6)$$

6) Summary of the obtained constraints: The constraints on $\sigma^2(\Lambda_{Q_i})$ and R_{q_i} reduce to the achievable quantization rate region given by (2)-(3) and

$$\sigma^2(\Lambda_{Q_i}) = \beta_i^2 \max\{\sigma^2_{1i}, \sigma^2_{2i}\} + \sigma^2(\Lambda_{cQ_i}). \quad (7)$$

Let $(R^*_{q_1}, R^*_{q_2})$ be a quantization rate couple satisfying the constraints (2)-(3). Using the definition of R_{q_i} and (7), one obtains $\sigma^2(\Lambda_{cQ_i}) = \frac{\beta_i^2 \max\{\sigma^2_{1i}, \sigma^2_{2i}\}}{2^{2R^*_{q_i}} - 1}$. Replacing these values into (6) and (5) concludes the proof of Proposition 1.

Note that the obtained results are independent from the choice of the γ_i and β_j parameters. However, these parameters impact the lattice choice.

7) Tunning γ_i and β_i: If we consider the analog signal transmission, since each relay performs compression, one has to minimize the obtained distortion at each user. Let us assume that the maximum allowed distortion for the reconstruction of the estimate of $\{U_{ij}\}_{i\in\{1,2\}}$ is defined as D_j.

Since both quantization indexes are recovered separately at each user, one has to study four distortions given by $D_{ij} = (\gamma_{ij}\beta_j - 1)^2\sigma_{ij}^2 + \gamma_{ij}^2\sigma^2(\Lambda_{cQ_j})$ and to verify that $D_1 \geq \max\{D_{21}, D_{11}\}$ and $D_2 \geq \max\{D_{22}, D_{12}\}$. One can prove that the minimal distortions are given by $D_{ij}^* = \frac{\sigma_{ij}^2\sigma^2(\Lambda_{cQ_j})}{\sigma^2(\Lambda_{cQ_j})+\beta_j^2\sigma_{ij}^2}$. Set $D_1 = \max_i\{D_{i1}^*\}$ and $D_2 = \max_j\{D_{j2}^*\}$ and let i^*, resp. j^*, denote $i^* = \arg\max_i\{D_{i1}^*\}$, resp. $j^* = \arg\max_j\{D_{j2}^*\}$.

The choice $\beta_1 = \gamma_{i^*1}^*$ and $\beta_2 = \gamma_{j^*2}^*$ yields $\beta_1 = \sqrt{1-\frac{D_1}{\sigma_{i^*1}^2}}$ and $\beta_2 = \sqrt{1-\frac{D_2}{\sigma_{j^*2}^2}}$. Note that in this case, $\sigma^2(\Lambda_{cQ_1}) = D_1$ and $\sigma^2(\Lambda_{cQ_2}) = D_2$, which is usually chosen for CF applied to the Gaussian relay channel.

B. Proof of Proposition 3

The proof is inspired by [12], where a lattice-based CF is proposed over the Gaussian relay channel. Encoding at user U_1, relay R_2 and the quantization step are done as previously with $\sigma^2(\Lambda_{cQ_2}) = D$ and $\beta_2 = 1$. Recall that $X_{R_1}(b) = \rho_1 X_1(b-1) + \rho_2 X_2(b-1) + \rho_3 Z_{R_1}(b-1)$.

1) Decoding at user U_i: As for CF/CF, the decoding at both users is done in a Wyner-Ziv fashion as depicted in Fig. 5. We briefly present the decoding steps at user U_1, decoding at user U_2 is done in a similar way. During block b, user U_1 starts by removing its own message, decodes the quantization index, removes it to form the side information $Y_{1,SI}(b) = h_1\rho_2 X_2(b-1) + Z_{eq_1}$, where $Z_{eq_1}(b) = h_1\rho_3 Z_{R_1}(b-1) + Z_1(b)$ is an equivalent Gaussian noise of power $N_{eq_1} = h_1^2\rho_3^2 N_{R_1} + N_1$. It then forms $\widehat{U}_{12}$ and MRC is used to combine the two noisy observations $\widehat{U}_{12}(b-1)$ and $Y_{1,SI}(b)$ of $X_2(b-1)$.

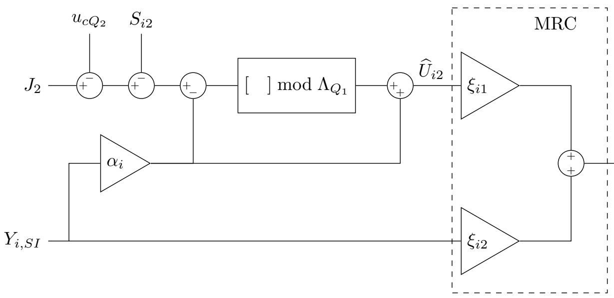

Fig. 5. Decoding of $X_{i'}$

All these steps are possible as long as

$$R_q \leq \min\left\{C\left(\frac{g_1^2 P_{R_2}}{N_{eq_1}+h_1^2\rho_2^2 P_2}\right); C\left(\frac{g_2^2 P_{R_2}}{N_{eq_2}+h_2^2\rho_1^2 P_1}\right)\right\}$$

$$\sigma^2(\Lambda_{Q_2}) \geq \max\left\{\frac{g_2^2 P_2 N_{eq_1}}{h_1^2\rho_2^2 P_2 + N_{eq_1}}; \frac{g_1^2 P_1 N_{eq_2}}{h_2^2\rho_1^2 P_1 + N_{eq_2}}\right\} + N_{R_2} + D$$

$$R_i^g \leq C\left(\frac{g_i^2 P_i}{N_{R_2}+D} + \frac{h_{i'}^2\rho_i^2 P_i}{N_{eq_{i'}}}\right).$$

2) Summary of the obtained constraints: All obtained constraints on R_q and $\sigma^2(\Lambda_{Q_2})$ reduce to

$$D \geq \frac{N_{R_2} + \max\left\{\frac{g_1^2 P_1 N_{eq_2}}{h_2^2\rho_1^2 P_1 + N_{eq_2}}; \frac{g_2^2 P_2 N_{eq_1}}{h_1^2\rho_2^2 P_2 + N_{eq_1}}\right\}}{\min\left\{\frac{g_1^2 P_{R_2}}{N_{eq_1}+h_1^2\rho_2^2 P_2}; \frac{g_2^2 P_{R_2}}{N_{eq_2}+h_2^2\rho_1^2 P_1}\right\}}.$$

Since both user's rate constraints are decreasing functions of D, the distortion has to be set with equality in order to maximize both user's rate, which concludes the proof. Note that in this case, $\sigma^2(\Lambda_{Q_2})$ is set as $\sigma^2(\Lambda_{Q_2}) = N_{R_2} + D + \max\left\{\frac{g_1^2 P_1 N_{eq_2}}{h_2^2\rho_1^2 P_1 + N_{eq_2}}; \frac{g_2^2 P_2 N_{eq_1}}{h_1^2\rho_2^2 P_2 + N_{eq_1}}\right\}$.

VI. Numerical Results

In this section, we present some numerical results. We suppose that both users are a unit distance apart, and that relay R_i is at a distance d_i from user U_1. The channel gains are given as $h_1 = \frac{1}{d_1^{3/2}}, h_2 = \frac{1}{(1-d_1)^{3/2}}, g_1 = \frac{1}{d_2^{3/2}}, g_2 = \frac{1}{(1-d_2)^{3/2}}$, following a common pathloss model.

Fig. 6 gives the achievable sum-rate as a function of d_1 and d_2 under CF/CF relaying (left) as well as the gap to the achievable sum-rate of [1, Corollary 1] (right), where each user chooses to send only over the best relay. Similarly, Fig. 7, resp. Fig. 8, presents the achievable sum-rate under DF/CF, resp. AF/CF, relaying, as well as the gap to the achievable sum-rate of [1, Corollary 1].

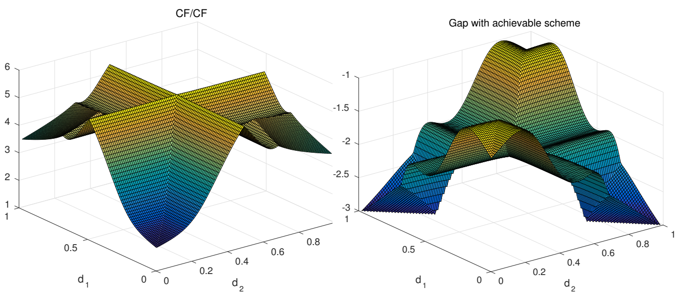

Fig. 6. CF/CF with $P_{R_i} = P_i = 10, N_{R_i} = N_i = 1$, Achievable sum-rate in bits (left) and gap to the achievable rate of [1, Corollary 1] (right) in bits

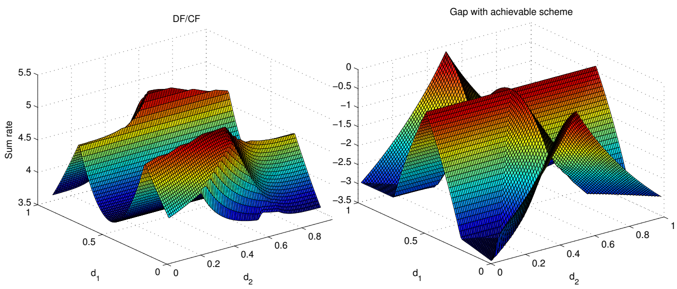

Fig. 7. DF/CF with $P_{R_i} = P_i = 10, N_{R_i} = N_i = 1$, Achievable sum-rate in bits (left) and gap to the achievable rate of [1, Corollary 1] (right) in bits

What is remarkable is that exploiting both relays always provides a better performance to the users as compared to the

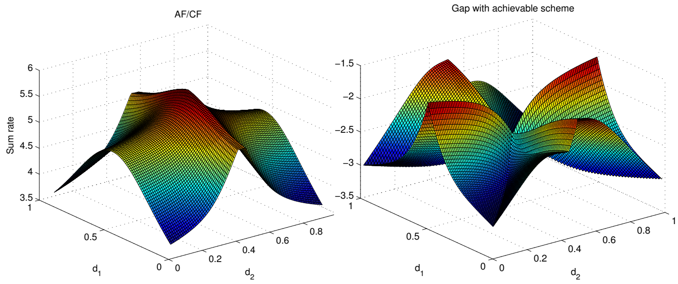

Fig. 8. AF/CF with $P_{R_i} = P_i = 10, N_{R_i} = N_i = 1$, Achievable sum-rate in bits (left) and gap to the achievable rate of [1, Corollary 1] (right) in bits

case in which only the relay yielding the best individual rate is used [1, Corollary 1]. As for the Gaussian relay channel, the Gaussian two-way relay channel or the multi-way relay channel, none of the relaying scheme is optimal for all channel gains and the three proposed relaying schemes can outperform the others for a specific set parameters (e.g. relays' positions), which results in very different shapes of the achievable sum-rates.

Recall that for the Gaussian relay channel, DF outperforms AF and CF when the relay is close to the user, whereas CF outperforms DF and AF when the relay is close to the destination. AF always gives the worst performance, but it achieves it's maximum rate when the relay is in the middle. Similar observations can be made for the Gaussian two-way relay channel without direct links: DF outperforms AF and CF when the relay is close to one user, whereas CF outperforms DF and AF when the relay is somewhere in the middle. Also, when the relay is close to one user, AF achieves higher sum-rate than CF, but lower than DF, and when the relay is somewhere in the middle, AF achieves higher sum-rates than DF, but lower than CF. All these well-known results will allow to give some insights on why the proposed schemes over the Gaussian TWDRC are better for some relay positions.

For the Gaussian TWDRC, AF/CF achieves high sum-rates compared to other schemes when both relays are in the middle, which is a direct consequence of the good performance of both AF and CF over the Gaussian two-way relay channel for these relays' positions. CF/CF also performs well in this region, which again can be easily explained following the same argument. For DF/CF, one can note a large sum-rate decrease in this region, which comes from the activation of the MAC sum-rate constraint for DF, as for instance over the Gaussian two-way relay channel.

DF/CF achieves high sum-rates when relay R_1 is closer to user U_1 and relay R_2 almost in the middle, closer to user U_2, or reverse. A position of R_1 close to U_1 allows a decoding of the message from user U_1 at high rate, and the position of relay R_2 almost in the middle closer to U_2 a compression of the message from user U_2 at high rate, which explain the good performance of DF/CF in this region. On the other hand, neither CF nor AF performs well when the relay is closer to one user, which explains the poor performance of AF/CF and CF/CF in this region.

CF/CF achieves high sum-rates when relay R_1 is close to user U_2 and relay R_2 close to user U_1, or reverse. For this set of relays' positions, both compression from user U_1 to user U_2 and from U_2 to user U_1 are performed at high rate. In this region, both DF/CF and AF/CF perform poorly: DF/CF because one scheme, either CF or DF, can be performed at high rate while the other is performed at very low rate and AF because of its lack of efficiency for these relays' positions.

VII. Conclusion

In this paper, we studied three relaying schemes over the Gaussian two-way diamond relay channel when relay R_2 uses a lattice-based CF scheme and relay R_1 uses either a lattice-based CF, DF or AF. For all relaying schemes, we characterized the achievable rate region and compared their performance via numerical illustrations. For future work, achievable rate regions where relay R_2 performs other schemes than CF, as for instance DF or AF, should be characterized, allowing for a comparative study of performance. Even if it is rather unlikely that one specific relaying scheme will perform better than all other schemes for all channel setups, conclusions could be drawn for specific positions of the relays.

Acknowledgment

This work has been partly funded by the French national agency for research under grant n^o ANR-16-CE25-0001.

References

[1] M. Ashraphijuo, V. Aggarwal, and X. Wang, "On the capacity regions of two-way diamond channels," *IEEE Trans. on Inform. Theory*, vol. 61, no. 11, pp. 6060 – 6090, Nov. 2015.

[2] T. M. Cover and A. E. El Gamal, "Capacity theorems for the relay channel," *IEEE Trans. on Information Theory*, vol. 25, no. 5, pp. 572–584, Sep. 1979.

[3] P. Hu, C. Sung, and K. Shum, "Joint channel-network coding for the gaussian two-way two-relay network," *EURASIP Journal on Wireless Communications and Networking*, Dec. 2010.

[4] B. Nazer and M. Gastpar, "Compute-and-forward: harnessing interference through structured codes," *IEEE Trans. on Information Theory*, vol. 57, no. 10, pp. 6463–6486, Oct. 2011.

[5] M. Nokleby and B. Aazhang, "Lattice coding over the relay channel," *IEEE International Conference on Communication (ICC)*, 2011.

[6] G. Poltyrev, "On coding without restrictions for the AWGN channel," *IEEE Trans. on Information Theory*, vol. 40, no. 2, pp. 409–417, Mar. 1994.

[7] V. Prathyusha, B. Srikrishna, and T. Andrew, "The Gaussian two-way diamond channel," *Allerton*, pp. 1292–1299.

[8] C. A. Rogers, "Lattice coverings of space," *Mathematica*, vol. 6, pp. 33–39, 1959.

[9] A. Savard and C. Weidmann, "Lattice coding for the gaussian one- and two-way relay channels with correlated noises," *IEEE International Symposium Information Theory (ISIT)*, 2015.

[10] ——, "On the gaussian multiway relay channel with intra-cluster links," *EURASIP Journal on Wireless Communications and Networking, SpringerOpen*, vol. 52, pp. 1–17, 2016.

[11] S. Smirani, M. Kamoun, M. Sarkiss, A. Zaidi, and P. Duhamel, "Achievable rate regions for two-way relay channel using nested lattice coding," *IEEE Trans. on Wireless Communications*, Jun. 2014.

[12] Y. Song and N. Devroye, "Lattice codes for the Gaussian relay channel: Decode-and-forward and compress-and-forward," *IEEE Trans. on Information Theory*, vol. 59, no. 8, pp. 4927 – 4948, Aug. 2013.

[13] E. C. van der Meulen, "Three-terminal communication channels," *Adv. Appl. Prob.*, vol. 3, pp. 120–154, 1971.

[14] R. Zamir, "Lattices are everywhere," *Proc. Inf. Theory Appl. Workshpop, La Jolla, CA*, pp. 392–421, 2009.